Journal of Optoelectronics and Advanced Materials Vol. 7, No. 5, October 2005, p. 2753 - 2762

SOL-GEL DERIVED IRON OXIDE-SILICA NANOCOMPOSITES, STARTING FROM IRON CHLORIDE AND IRON NITRATE

M. Popovici[a], C. Savii[a*], C. Enache[a], D. Niziiansky[b], I. Subrt[b], E. Vecemikova[b]

[a]Romanian Academy - Timisoara Brh., Inorganic Chemistry Lab., 24 Mihai Viteazul Blvd., 1900 Timisoara, Romania
[b]Academy of Sciences of the Czech Republic, Institute of Inorganic Chemistry, Dept. of Solid State Chemistry, 250 68 Ref, Czech Republic

Sol-gel Fez03-SiOz composites have been obtained, using tetraethoxysilane as precursor and ferric salts (chloride and nitrate), for a target composition of 32 wt. % Fe_20_3. The samples were characterized by thermal analysis, transmission electron microscopy, electron diffraction and X-ray diffraction. Mossbauer spectroscopy showed that some of the resulting materials possess superparamagnetic and ferrimagnetic properties, indicating a distribution of particles size in nanometer and tens of nanometers range. The different results obtained suggest that the formation of iron oxide phases depends on the precursors employed and the atmosphere of thermal treatment.

(Received November 3, 2004; accepted September 22, 2005)

Keywords: Sol-gel processing, Nanophase-materials, Mössbauer spectroscopy

1. Introduction

Iron oxide-silica composites have been extensively studied in the last few years [1,2], due to potential applications in magnetic technology [3-5], catalysis [6], sensors [7-9], optics [10]. The SiOz matrix structure plays the role of host for iron oxide fine particles, which nucleates in the silica pores, conveniently obtained by controlled hydrolysis and condensation reactions of a silicon alcoxide. The pore size of the matrix imposes an upper limit on the iron oxide particles size and minimizes their aggregation.

The sol-gel derived materials are sensitive to many factors like H_2O/TEOS ratio, solvent/TEOS ratio, pH, additives or thermal conditions during sol to gel transition. The structure and properties of iron oxide developing phases in a silica matrix depend on nature of the anion present in solution. Flynn has reviewed the results obtained by different authors concerning the hydrolysis behavior of aqueous solutions of ferric salts (chloride, perchlorate, sulphate, nitrate, phosphate). It is reported that, while the NO_3^- is not coordinated to the iron (III), the chloride ion is retained in Fe^{3+} aquocomplexes species [11].

Del Monte and collaborators reported a comparative study of iron oxide formation in a silica matrix using chloride and nitrate salts as sources of ferric ions in ethanol solution. The gamma oxide phase was obtained in case of the nitrate salt and the alpha oxide phase in the case of the chloride [12]. Other studies report the formation of hematite [13-17] or maghemite, which can be lately converted at higher temperatures in hematite [18-21]. The obtained results are quite different due, probably, to high sensitivity of the sol-gel process relative to working parameters (precursors, solvent, concentration, pH, thermal treatment).

Silica matrices have a stabilizing effect over maghemite nanoparticles with dimension generally less than 10 nm with superparam~gnetic behavior [127].

We choose to see what kind of iron phases are supposed to be formed using a certain

* Corresponding author: cecilias@acad-icht.tm.edu.ro

hydrolysis ratio and thermal treatment in air or vacuum atmosphere, at fixed concentration of iron oxide. For this purpose, acid catalyzed hydrolysis and condensation of tetraethoxysilane was employed. The composites obtained by thermal treatment of derived gels, in air, respectively in vacuum, were characterized by thermogravimetric and differential thermal analyses, X-ray diffraction and transmission electron microscopy and Mössbauer spectroscopy.

2. Experimental

The sol-gel syntheses were conducted for a target composition of 32 wt. % wt.Fe_20_3 at fixed hydrolysis ratio. The sols were prepared by dissolving ferric chloride hexahydrate (Peking Chemical Works, 99%) or ferric nitrate nonahydrate (Riedel-de Haen, 96%) in a mixture of water-ethanol and subsequently adding of tetraethoxysilane (Fluka, 98%) drop wise under continuous stirring for 20 minutes. The reaction pH was situated around 0.9. The formed wet gels were dried at 60 °C for 14 hours, then powdered and fired in 300-1100 °C range in air, with steps of 100 °C up to 1000 °C and kept 3 hours at maximum temperature. In order to evaluate the influence of fIring atmosphere upon the crystalline iron oxide phase formed in the system, the gels were also heat treated in vacuum up to 400 °C.

In the following, the annealed samples will be named as follows:

- chloride derived sample: C X (thermal treatment in air) or TC X (thermal treatment in vacuum);
- nitrate derived sample: A X (thermal treatment in air) or TA X (thermal treatment in vacuum);

X represents the thermal treatment temperature.

The resulted composite powders were fine crushed in a mortar and were characterized by using thermo gravimetric and differential thermal analyses coupled with mass spectrometry, X-ray diffraction (XRD), transmission electron microscopy (TEM) and Mössbauer spectroscopy.

3. Results

Nanocomposites obtained by thermal treatment in air (C900 and A900 samples)

Thermal analysis

The thermogravimetric and differential thermal analyses were recorded on a NETZSCH 409/429-403/QMS apparatus in air flow using alumina crucible; heating was carried out in the range 20-1000 ^oC at a rate of 10 ^oC/min. The results obtained for C (chloride derived sample) and A (nitrate derived sample) are presented in Fig. 1 and Fig. 2, respectively.

Thermogravimetric analyses have shown that the main mass loss occurs almost continuously up to 400 ^oC (48.3 % for the C sample and 28.3 % for the A sample). This effect registered on TG curves can be firstly assigned to removal of water, solvent and to organics carbonization, being associated with a large endothermic effect marked on DTA curve. Some further qualitative details may be deduced from the TG-MS data. The release of water occurs with maximum intensity at 191 ^oC for C sample, about 10 ^oC above the maximum recorded in the case of A sample, and more, a weak shoulder at 243 ^oC being evidenced in case of ferric chloride derived sample. This must be due to removal of hydroxyl groups strongly bonded in structure. In fact, chloride salt retains three times much water in structure (estimated from MS peak areas), fact that have confirmed the observation of del Monte [12]. The exothermic effects at 439 ^oC (C sample) and 480 ^oC (A sample) are probably the result of carbon containing groups oxidization (MS spectra).

The chloride (C sample) removal begins around 300 ^oC, having the maximum intensity at 415 ^oC.

The nitrate decomposition (A25 sample) takes place at lower temperatures, in 230-240 ^oC range (fragments detected at m/z=29, NO, and m/z=46, NO_2). In this case the DTA curve shows a prolonged shoulder, due to the superimposed effects of oxidative processes related to CO_2, NO and NO_2 formation.

At higher temperatures than 600 °C, the broad exothermic effect could be the result of conversion of amorphous iron oxide to crystalline state [19].

X-ray diffraction

The crystalline phases obtained in the composites were identified by X-ray diffraction, in a Siemens D 5005 X-ray powder diffractometer, with diffracted beam monochromator, using CuKα radiation. The pattern was recorded from 10° to 90° with a step size of 0.1° and a scanning rate of 15 s per step.

X-ray diffraction investigations have revealed that the samples heat treated in air at temperatures up to 600 °C do not show any signal of crystalline phase. Beginning with this temperature from the amorphous background emerge very broad diffraction lines due to weak crystallinity and/or very small dimension of the iron oxide crystalline particles.

In both XRD patterns of samples fired at 900 °C (Fig. 3) at small angle region (22-27o) appears a broad maximum due to amorphous character of silica matrix.

X-ray diffraction pattern of the C 900 sample (derived from ferric chloride and fired at 900 °C) presents well developed diffraction peaks that can be undoubtedly ascribed to hematite (α-Fe_2O_3), with an average particles size of ~75 nm derived from line broadening using Scherrer formula.

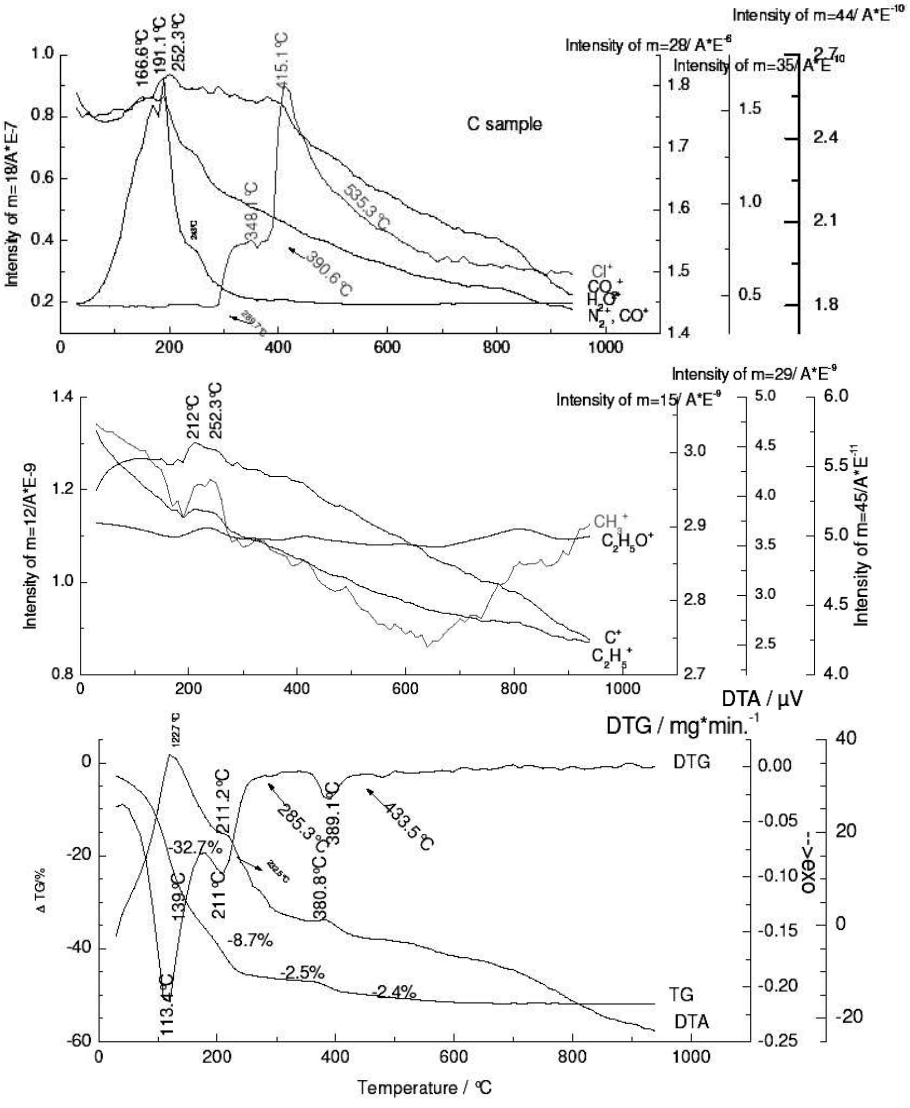

Fig. 1. Thermal evolution of C sample.

In the case of A 900 sample (derived from ferric nitrate and also fired at 900 °C), the typical features of a nanocrystalline material with weak and broader diffraction lines are observed. The main features of ε-Fe_2O_3 phase could be observed, but also the diffraction lines of hematite are present. X-ray diffraction peaks attributed to epsilon phase were indexed using different sets of data (JCPDS 16-0895, 16-0653), but significant variations in the intensities are observed. Our epsilon phase X-ray diffraction lines better match with the pattern proposed by Tronc et al. [24]. The average particle size of 21 nm was deduced from the line broadening of the diffraction peaks using the Scherrer formula, where l=1.5406 (CuKα) and K=0.89.

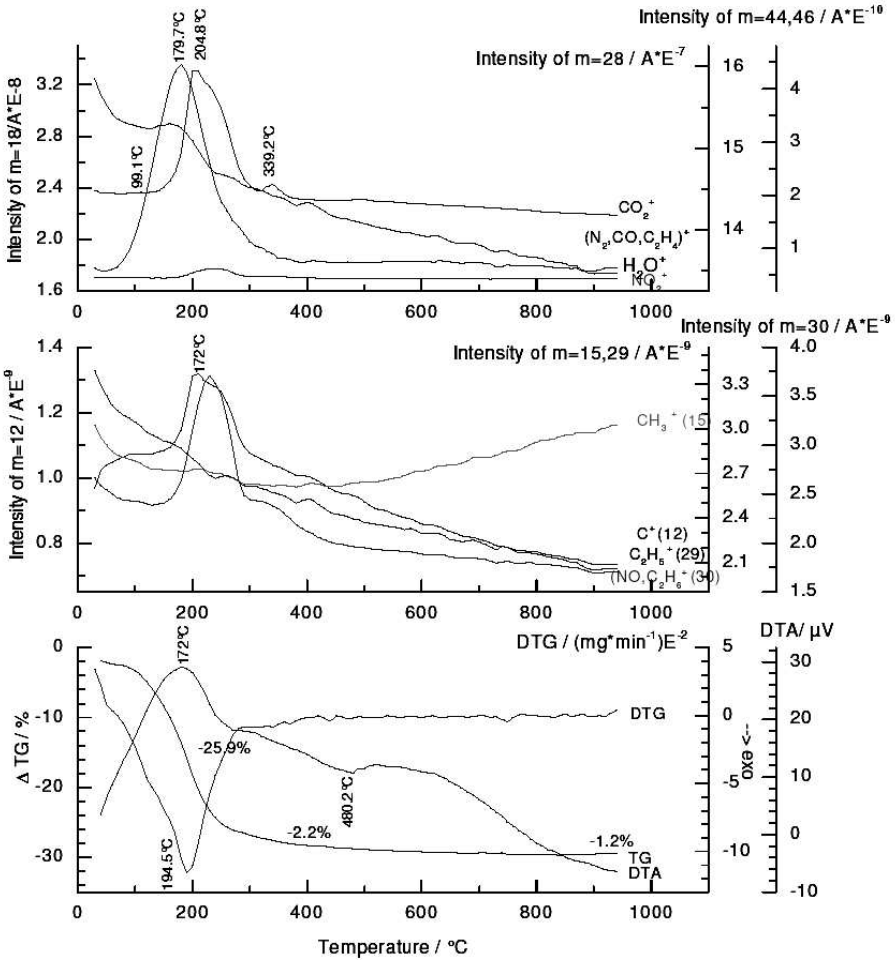

Fig. 2. Thermal evolution of A sample

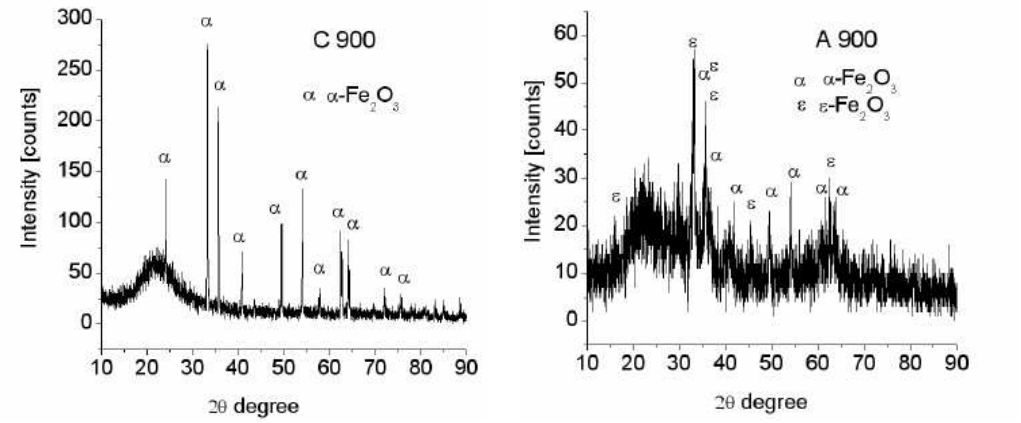

Fig. 3. XRD patterns of C 900 and A 900 samples.

Transmission electron microscopy

Transmission electron microscopy of the two samples shows a heterogeneous distribution of particle size some very large with ~100 nm diameter (Fig. 4a) and some very small with mean iameter of 6.9±1.0 nm (Fig. 4b), in the case of C900 sample and 20±2.5 nm for A900 sample (Fig. 4 c).

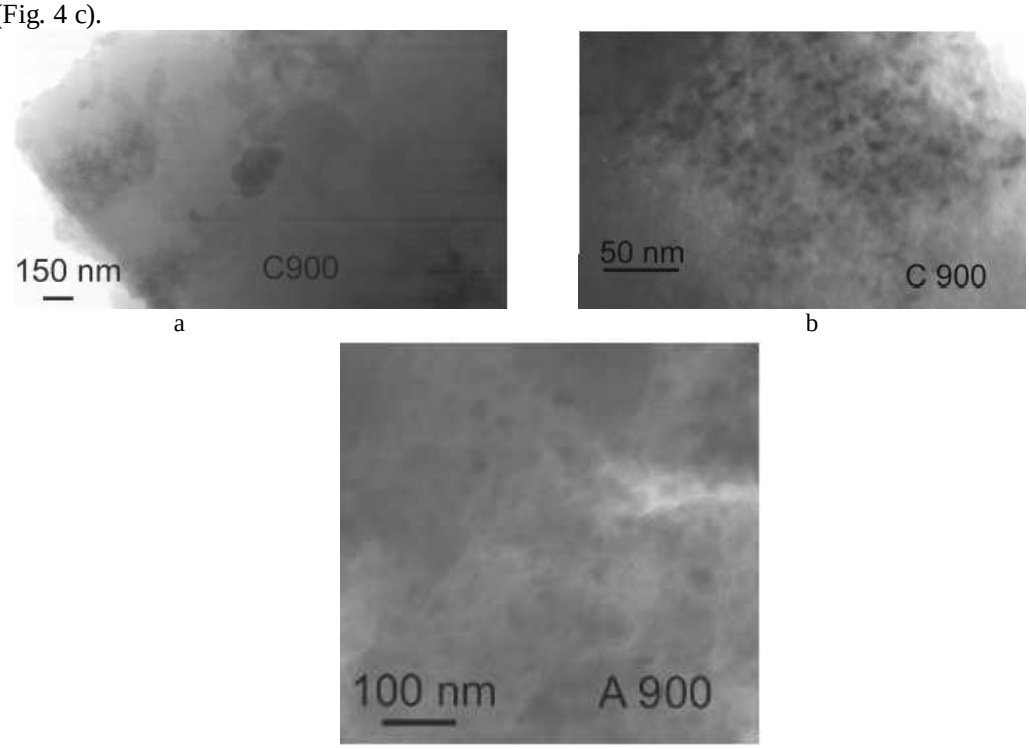

a b c

Fig. 4. TEM micrographs a) and b) of C900 sample and c) of A900 sample.

Electron diffraction patterns

Electron diffraction patterns of C900 (Fig. 5) samples are characteristic either to very large particles (Fig. 5a), or consist from rings revealing very small particles (Fig. 5b), both ascribed to hematite. In the Fig. 5c, electron diffraction pattern of A900 sample consist of point rings and isolated point, showing small particles in nanocrystalline state, assigned to epsilon ferric oxide and to hematite.

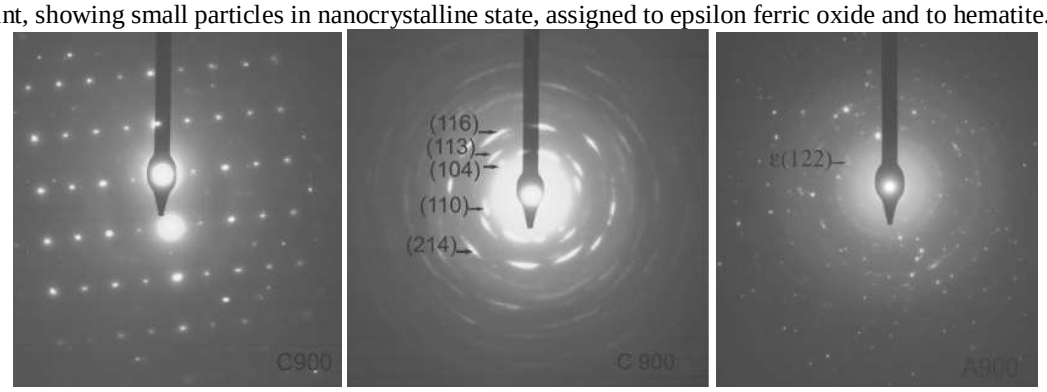

Fig. 5. Electron diffraction patterns of C 900 sample (a,b), and A 900 sample (c)

In the Fig. 5, electron diffraction pattern of A900 sample, consist of rings which are constituted from points indicating the presence of small particles in nanocrystalline state. The characteristic planes of epsilon and alpha phase of iron oxides were both identified.

Mössbauer spectroscopy

Mössbauer spectra were carried out at room temperature. The all isomer shifts are consistent with Fe^{3+}.The sample C900, C1000 and C1100 (Fig. 6) have the characteristic sextet of hematite and a doublet due to a small amount of para- (or superpara-) magnetic phase. The A900, A1000 and A1100 are more complex spectra (Fig. 7) which can be decomposed in 5 sextets (epsilon phase and alpha phase of iron oxide) and two doublets. The spectral parameters are shown in Table 1.

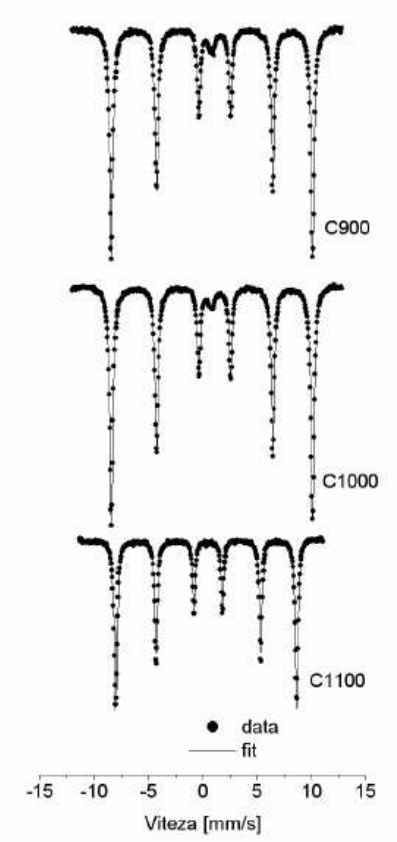

Fig. 6. Mössbauer spectra of C900, C1000 and C1100 samples.

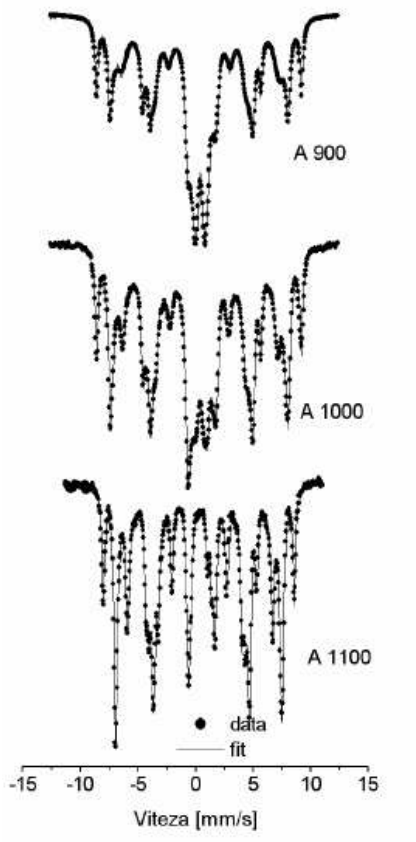

Fig. 7. Mössbauer spectra of A900, A1000, and A1100 samples.

The Mössbauer spectrum of C 900 sample is composed from one sextet with a quadrupole splitting –0.21 mm/s and a hyperfine field of 51.7 T, both spectral parameters being characteristic to hematite. The second subspectrum with weak relative intensity about 4% is due to a small proportion of iron in disordered state or having small crystallite size around few nanometers, fact confirmed by the absence of hyperfine magnetic splitting. The fitting of Mössbauer spectra was realized by means of broad sextet in case of epsilon phase. Improved fits of these spectra were realized using Gaussian distribution of the Lorentzian (Voigt profiles).

The Mössbauer spectrum of A 900 sample can be fitted by five sextets and two doublets. The first sextet could be ascribed to hematite (9%) in base of hyperfine field about 51.6 T. The next four sextets having hyperfine field values of 44.9 T, 42.9, 39.4 T and 26.6 T are characteristic to ε-Fe_2O_3 phase (~ 50 %). For ε-Fe_2O_3 were reported three octahedral sites, two of them characterized by similar values (~ 45 T) of hyperfine field and a third one by smaller hyperfine field (~40 T). The tetrahedral site is characterized by hyperfine field of ~26 T. The two doublets could be attributed to paramagnetic (or magnetically ordered phase in superparamagnetic state) in base of large quadrupole splitting values which are known to increase with decreasing particle size and the absence of hyperfine magnetic field. The broad component is related to the fraction of nanoparticles in blocked state (14%) having dimensions slightly bigger than those corresponding to nanoparticles in

superparamagnetic state (27%). The Mössbauer spectra are also recorded for the A sample heat treated at 1000 and 1100 ^{o}C. Evaluating the spectral parameters of A 1000 and A 1100 samples, it can be observed that the hematite content remains approximately constant, and the fraction of superparamagnetic phase is diminishing to disappearance at 1100 ^{o}C. It seems that on the expenses of this amount of superparamagnetic particles, the amount of iron oxide nanoparticles in blocked state increase, due probably to the growing of particle size at elevated temperatures.

Table 1. Hyperfine parameters of the samples heat treated between 900-1100 ^{o}C.

Sample	No. Subsp.	Relative area [%]	Isomer shift δ [mm/s]	Quarupole splitting ΔE_Q [mm/s]	Hyperfine field H_{hf} [T]
C 900	1	96	0.36	-0.21	51.7
	2	4	0.24	0.30	-
C 1000	1	96	0.36	-0.21	51.7
	2	4	0.22	0.17	-
C 1000	1	96	0.39	-0.19	51.7
	2	4	0.44	Broad component	-
A 900	1	9.8	0.38	-0.21	51.6
	2	13.8	0.37	-0.20	44.9
	3	8.2	0.38	-0.32	42.9
	4	16.6	0.37	-0.01	39.4
	5	11.6	0.19	-0.20	26.7
	6	26.8	0.34	0.81	-
	7	13.2	0.72	Broad component	-
A 1000	1	9	0.37	-0.19	51.5
	2	10.2	0.36	-0.17	45.0
	3	14.0	0.38	-0.27	43.8
	4	14.0	0.37	-0.02	39.1
	5	9.1	0.19	-0.19	26.0
	6	17.1	0.35	0.87	-
	7	26.6	0.47	Broad component	-
A 1100	1	9.7	0.37	-0.21	51.5
	2	8.4	0.36	-0.19	45.3
	3	18.7	0.37	-0.29	44.5
	4	16.6	0.37	-0.02	39.2
	5	13.2	0.21	-0.17	26.0
	6	33.4	0	Broad component	-

Nanocomposites obtained by thermal treatment in vacuum (TC400 and TA400)

X-ray diffraction

The patterns obtained by X-ray diffraction (Fig. 8) show that in the case of chloride derived sample TC 400, the XRD peaks have greater intensities. TA 400 sample is characterized by smaller and broader XRD peaks. It is rather difficult to assign the peaks to a certain iron oxide phase, due to very similar value of d-spacings. However, the diffraction lines of hematite are clearly observed in the case of chloride derived sample.

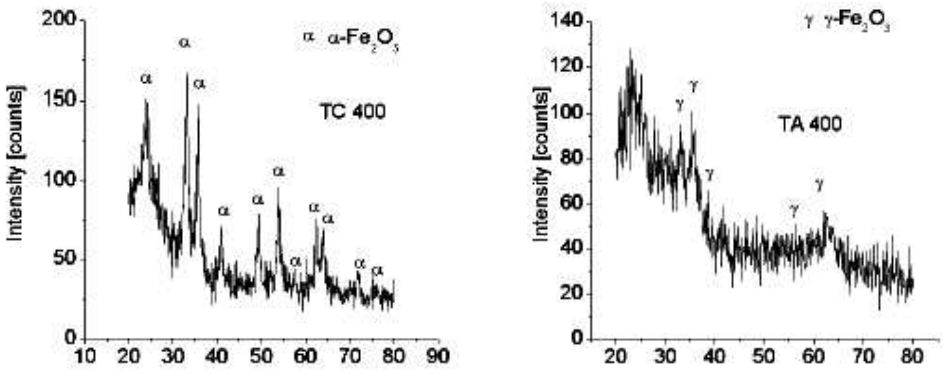

Fig. 8. XRD patterns of TC 400 and TA400 samples.

In the case of TA 400 sample, the main diffraction lines correspond to maghemite or magnetite, which is probably present, but the presence of hematite, is also not excluded. From the broadening of the diffraction lines results that the particles have a distribution of sizes in nanometer range with a mean diameter of 15 nm (TC 400), respectively 11 nm (TA 400).

Mössbauer spectroscopy

The Mössbauer spectrum of TC 400 sample (Fig.9), can be deconvoluted in two doublets having isomer shift values consistent with Fe^{3+} and four sextets characterized by a non-symmetric distribution of hyperfine field which is an indication for a broad distribution of particle sizes. Based on δ values of 0.36-0.38 mm/s and ΔE_Q~0.20-0.21 mm/s, the sextets are assigned to hematite phase. The smaller values of the hyperfine fields observed in comparison with the characteristic hyperfine field of 51.7 T for bulk hematite reveal the presence of very small particles situated in nanometer range (Table 2.).

In the case of TA 400 sample (Fig. 9) the presence of three doublets suggest that two of them correspond to the iron ions from the core of the nanoparticles, situated in nonequivalent sites (ΔE_Q = 0.54 mm/s, 0.90 mm/s) and third one correspond to iron at the surface of the particles (ΔE_Q = 1.34 mm/s). The two sextets are due to a small amount (11.8%) of the ordered iron ions having mixed valency of about Fe2.5+ (δ=0.40 mm/s) and different values of hyperfine field, which could be assigned to a small amount of iron oxide in spinel phase (magnetite) probably slightly distorted from cubic symmetry (ΔE_Q close to –0.1 mm/s).

Table 2. Hyperfine parameters of the samplea heat treated at 400 °C.

Sample	No. Subsp.	Relative area [%]	Isomer shift δ [mm/s]	Quarupole splitting ΔE_Q [mm/s]	Hyperfine field H_{hf} [T]
TC 400	1	4.3	0.36	0.66	-
	2	6.6	0.33	1.04	-
	3	32.4	0.36	-0.21	43.0
	4	18.2	0.37	-0.20	45.8
	5	28.5	0.38	-0.21	48.1
	6	10.0	0.38	-0.20	49.6
TA 400	1	28.8	0.34	0.54	-
	2	38.4	0.34	0.90	-
	3	21.0	0.33	1.34	-
	4	6.5	0.40	-0.14	43.6
	5	5.3	0.40	-0.10	48.1

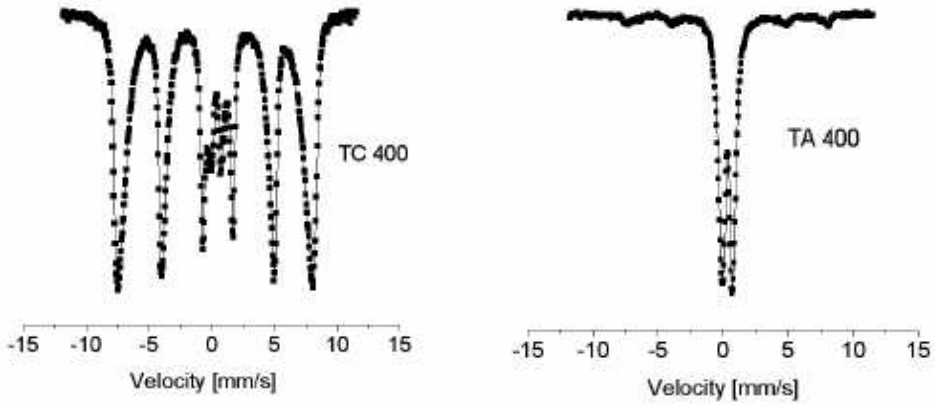

Fig. 9. Mössbauer spectra at room temperature of TC 400, and TA400 samples.

4. Discussion

In the light of the obtained results, it appears that used ferric precursors, influence the formation of certain iron oxide by thermal treatment. Probably, an important role is played by the polymerization processes of ferric ions that occur in the pore of silica matrix. Some previous studies related to structure and formation of polymers during hydrolysis of different ferric salts, reveal that in the case of chloride, the polymerization of Fe follows a set pathway including the formation of an intermediate polycation "Fe_{24}" whose local structure is that of akaganeite [25], whereas the growth of iron nitrate phases involves a variety of different subunits [26-30]. This fact was explained by Rose et al.[27]; in the case of ferric chloride solutions, in the early stages of hydrolysis and at low hydrolysis ratio, one or two Cl atoms remain in each octahedron, and from this reason not all nucleation sites for the polymerization of iron remain available. For ferric nitrate solution, all the potential binding sites are available, since each Fe is surrounded by six oxygens (OH groups or H_2O molecules). From this reason, there are many possibilities for further polymerization of iron atoms, in the case of hydrolysis of ferric nitrate salt.

We believe that an important role in formation of specific iron oxide phase is the atmosphere of thermal treatment. Del Monte and colab. [12] have shown that gamma phase is obtained up to 400 ^oC, probably as a results of reduction processes of organics present. By air thermal treatment, the reduction processes are avoided and iron ions remain in trivalent state. We have obtained crystalline phase only at temperatures higher than 700 ^oC, as it was reported by Cannas [2], but they reported that the iron oxide formed is gamma with possible presence of epsilon phase. From the X-ray data together with the Mössbauer ones, we suppose that in our case, the main iron oxide phase formed is epsilon ferric oxide, beside a small amount of hematite.

5. Conclusions

It was synthesized iron oxide nanoparticles dispersed in silica matrix composites. As result of different thermal treatments applied (vacuum up to 400 ^oC, or air up to 1100 ^oC) a different phase evolution can be remarked. By thermal treatment in air the crystalline phase appears at temperatures higher than 600 oC, but thermal treatment in vacuum favorises the synthesis of crystalline phases at relatively low temperatures (400 ^oC).The nature of iron salts also influence the crystalline phase formed. The chloride derived samples contain only antiferromagnetic hematite. The nitrate ions lead to formation of ferrimagnetic phases: mainly in ε-Fe_2O_3 (thermal treatment in air) or spinel phase (maghemite and/or magnetite, by thermal treatment in vacuum).

The investigations have shown that anions present influence the formation of α- or ε- phase in final composites. The particle size increase with temperature, the areas of the sextets corresponding to epsilon phase increase as a result of it. The analysis of Mössbauer spectral parameters show that the epsilon phase is stable even at 1100 ^oC, the amount of hematite formed in the system being approximately the same as at 900 ^oC.

From the X-ray data together with the Mössbauer ones, we suppose that in our case, the iron oxide directly formed from amorphous phase is epsilon ferric oxide, beside a small amount of hematite (around 8-10%). Iron oxide phase crystallizes in the case of thermal treatment in vacuum at 400 ^{o}C also as α-Fe_2O_3 (hematite) in the case of ferric chloride precursor, but the iron oxide derived from the ferric nitrate is Fe_3O_4 (magnetite).

Acknowledgements

This work is a part of the project no.6/2001 of NATO program of the Czech Republic and has been partially supported by Grant CNCSIS nr.32826/2004 (Romania) and by Contract No.1098/1997 – Add.No. 1/2004.

The authors thank Romanian Academy and Academy of Sciences of the Czech Republic.

References

[1] C. Cannas, D. Gatteschi, A. Musinu, G. Piccaluga, C. Sangregorio, J. Phys. Chem.B **102**, 7721(1998).
[2] C. Cannas, G. Concas, A. Musinu, G. Piccaluga, G. Spano, Z. Naturforch. **54a**, 513(1999).
[3] D. D. Awschalom, D. P. DiVicenzo, Phys. Today **43**, 56 (1995).
[4] R. F. Ziolo, E. P.Giannelis, B. A. Weinstein, M. P. O'Horo, B. N. Ganguly, V. Mehrotra, M.W. Russell, D. R. Huffman, Science **257**, 219 (1992).
[5] R. D. McMichael, R. D. Shull, L. J. Schwartzendruber, L. H. Benett, R. E. Watson, J.Magn.Magn.Mater. **111**, 29 (1992).
[6] T. Ida, H. Tsuki, A. Ueno, K. Tohoji, Y. Udagawa, K. Iwai, H. Sano, J. Catal. **106**, 428 (1987).
[7] C. Cantalini, M. Pelino, J.Am.Ceram.Soc. **75**, 546(1992).
[8] C. Cantalini, H. T. Sun, M. Faccio, G. Ferri, M. Pelino, Sensors and Actuators **B 24-25**, 673 (1995).
[9] H. T. Sun, C. Cantalini, M. Faccio, M. Pelino, M. Catalano, L. Tapfer, J. Am. Ceram. Soc. **79**, 927(1996).
[10] S. Roy, D. Das, D.Chakravorty, D. C. Agrawal, J. Appl. Phys. **74**, 4746 (1993).
[11] C. M. Flynn, Jr., Chem. Rev. **84**, 31(1984).
[12] F. del Monte, M. P. Morales, D. Levy, A. Fernandez, M. Ocana, A. Roig, E. Molins, K. O'Grady, C. J. Serna,_Langmuir **13**, 3627 (1997).
[13] M. Guglielmi, G. Principi, J. Non-Cryst. Solids **48**, 161 (1982).
[14] K. Tanaka, K. Kamiya, M. Matsuoka, T. Yoko, J. Non-Cryst.Solids 94, 356 (1987).
[15] I. Peleanu, M. Zaharescu, I. Rau, M. Crisan, A. Jitianu, A. Meghea, J. Radioanalytical and Nuclear Chemistry **246**, 557 (2000).
[16] M. Zaharescu, M. Crisan, A. Jitianu, D. Crisan, A. Meghea, I. Rau, J. Sol-Gel Science and Technology **19**, 631 (2000).
[17] M. Popovici, C. Savii, A. Gluhoi, R. Turcin, C. Enache, M. Turcu, C.Caizer, I.Hrianca, Proceedings of The IVth International Symposium "Regional Multidisciplinary Research", Romania-Yugoslavia-Hungary, 16-17 November 2000, S.C. Infotim S.A., Editura Sudura, Timisoara, ISBN: 99425-8–X, 2001, p.632.
[18] C. Cannas, D. Gatteschi, A. Musinu, G. Piccaluga, C. Sangregorio, J. Phys. Chem. **102**, 7721 (1998).
[19] G. Ennas, A. Musinu, G. Piccaluga, D. Zedda, D. Gatteschi, C. Sangregorio, J. L. Stanger, G. Concas, G. Spano, Chem. Mater. **10**, 495 (1998).
[20] I. Hrianca, C. Caizer, C. Savii, M. Popovici, J. Optoelectron. Adv. Mater. **2**, 634 (2000).
[21] C. Cannas, G. Concas, D. Gatteschi, A. Falqui, A.Musinu, G.Piccaluga, C. Sangregorio, Phys. Chem. Chem. Phys. **3**, 832 (2001).
[22] C. Caizer, M. Popovici, C. Savii, Ann. West Univ. Timisoara, Ser.Fiz. **43**, 124 (2002).
[23] C. Caizer, C. Savii, M. Popovici, Mater. Sci. Eng. B **97**, 129 (2003).
[24] E. Tronc, C. Chaneac, J. P. Jolivet, Journal of Solid State Chemistry **139** , 93 (1998).
[25] S. Solinas, G. Piccaluga, M. P. Morales, C. J. Serna, Acta Materialia **49**, 2805 (2001).
[26] J. Y. Bottero, D. Tchoubar, M. Arnaud, P. Quienne, Langmuir **7**, 1365 (1991).
[27] J. Rose, A. Manceau, A. Masion, J. Y. Bottero, Langmuir **13**, 3240 (1997).
[28] U. Schwertmann, J. Friedl, G. Pfab, J. Solid State Chem. **126**, 336 (1996).
[29] U. Schwertmann, J. Friedl, H. Stanjek, J. Colloid Interface Sci. **209**, 215 (1999).